frontiers | Frontiers in Materials

ORIGINAL RESEARCH
published: 26 April 2022
doi: 10.3389/fmats.2022.877683

Electrochemical Studies of LbL Films With Dawson Type Heteropolyanion Glassy Carbon Electrode Sensor Modified for Methyl Parathion Detection

Nafeesa Allah Ditta[1], Mustansara Yaqub[2], Sohail Nadeem[1], Sundas Jamil[1], Sadaf Ul Hassan[1], Shahid Iqbal[3]*, Mohsin Javed[1], Eslam B. Elkaeed[4], Fwzah H. Alshammari[5], Norah Alwadai[6], Rami M. Alzhrani[7], Nasser S. Awwad[8] and Hala A. Ibrahium[9,10]*

[1]Department of Chemistry, School of Science, University of Management and Technology, Lahore, Pakistan, [2]Interdisciplinary Research Centre in Biomedical Materials, COMSATS University, Lahore Campus, Lahore, Pakistan, [3]Department of Chemistry, School of Natural Sciences (SNS), National University of Science and Technology (NUST), Islamabad, Pakistan, [4]Department of Pharmaceutical Sciences, College of Pharmacy, AlMaarefa University, Riyadh, Saudi Arabia, [5]Department of Physics, University Colleges at Nairiyah, University of Hafr Al Batin (UHB), Nairiyah, Saudi Arabia, [6]Department of Physics, College of Science, Princess Nourah Bint Abdulrahman University, Riyadh, Saudi Arabia, [7]Department of Pharmaceutics and Industrial Pharmacy, College of Pharmacy, Taif University, Taif, Saudi Arabia, [8]Chemistry Department, Faculty of Science, King Khalid University, Abha, Saudi Arabia, [9]Biology Department, Faculty of Science, King Khalid University, Abha, Saudi Arabia, [10]Department of Semi Pilot Plant, Nuclear Materials Authority, El Maadi, Egypt

OPEN ACCESS

Edited by:
Muhammad Sufyan Javed, Jinan University, China

Reviewed by:
Muhammad Saleem, Islamia University of Bahawalpur, Pakistan
Awais Ahmad, University of Córdoba, Spain

***Correspondence:**
Sohail Nadeem
sohail.nadeem@umt.edu.pk
Shahid Iqbal
shahidgcs10@yahoo.com

Specialty section:
This article was submitted to Polymeric and Composite Materials, a section of the journal Frontiers in Materials

Received: *17 February 2022*
Accepted: *21 March 2022*
Published: *26 April 2022*

Citation:
Ditta NA, Yaqub M, Nadeem S, Jamil S, Hassan SU, Iqbal S, Javed M, Elkaeed EB, Alshammari FH, Alwadai N, Alzhrani RM, Awwad NS and Ibrahium HA (2022) Electrochemical Studies of LbL Films With Dawson Type Heteropolyanion Glassy Carbon Electrode Sensor Modified for Methyl Parathion Detection. Front. Mater. 9:877683. doi: 10.3389/fmats.2022.877683

Rapid methyl parathion detection was measured using a fabricated glassy carbon electrode (GCE) sensor designed using the layer-by-layer (LBL) method. Multilayer assemblies were developed on the glassy carbon electrode by alternating depositions of anions and cations in which a Dawson Type Polyoxometalate β-$K_6[(P_2W_{18}O_{62}{\cdot}H_2O)]{\cdot}14H_2O$ (~P_2W_{18} POM) and polyethyleneimine (PEI) stabilized silver nanoparticles (~PEI-AgNPs) acted as anions and cations, respectively. The redox behavior of P_2W_{18} POM within LBL assembly was carried out *via* cyclic voltammetry. This LBL assembly was thoroughly characterized by UV-Visible, FT-IR, XRD, AFM, and SEM techniques. The fabricate GCE sensor was investigated for the electrocatalytic activity to detect methyl parathion. The results clearly showed that the fabricated GCE sensor was successfully synthesized. More interestingly, the current response for detecting methyl parathion was found to be less than 1 ppm, proving that this fabricated GCE sensor may exhibit potential applications in the detection of targeted pesticide.

Keywords: heteroloyanions, PEI-AgNPs, alternative multilayers, glassy carbon electrode, methyl parathion

1 INTRODUCTION

Pesticides play a vital role in different fields, being used as in the agricultural field for pest and weed control (Hussain et al., 2020) and for harvesting crops (Zheng et al., 2020), in homeland security, as a warfare agent, and also in food security (Facure et al., 2017). Pesticides contain a chemical used to kill unwanted organisms that can be present in different public places, i.e., gardens and agricultural areas (Hassaan and El Nemr, 2020). Among worldwide used pesticides, which are applied to control pests, approximately 36% belong to the organophosphorus pesticide class (Oultaf et al., 2022). Pesticides

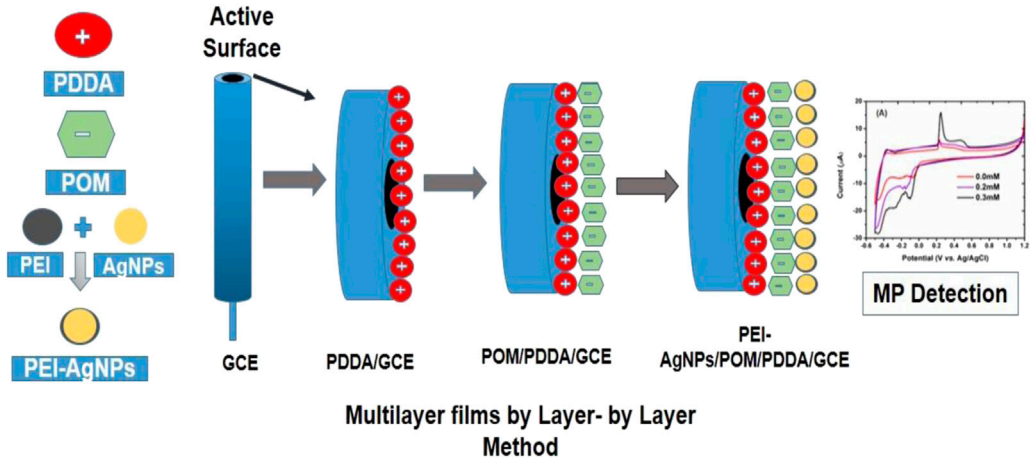

Graphical Abstract |

have the potential to decrease losses in crop production, especially from pests. Therefore, a pesticide is an integral part of crop production (Van Den Berg et al., 2022). Some pesticides exhibit photochemical transformation reactions for producing metabolites that have nontoxic effects on the environment and human health (Aktar et al., 2009). Pesticides have been manufactured all over the world, however, the United States is the top supplier of pesticides with ten billion tons of pesticides' production per annum. One-third of global crops are spoiled during harvesting, growth, and stowing without pesticides (Parham and Rahbar, 2010). Some pesticides in combined form have specific harmful effects on living organisms such as cancer and endocrine disorders (Sousa et al., 2020), neurological diseases, immune system destruction, ocular or endocrine disruption, and dermal disorders (Negatu et al., 2016). In 1970, organophosphate pesticides were introduced in the market, and they are now the largest class of pesticide. The compounds which contain phosphorous are called organophosphate (OPs) (Febbraio et al., 2011). Organophosphates (OP) have nitro-phenyl groups or halogens (which are electrochemically active compounds). There are some methods for detecting methyl parathion. Among them, traditional methods for detecting MP include analytical methods i.e., gas chromatography-mass spectrometry (GC-MS), liquid chromatography (LC) (Luo et al., 2021), fluorescence, capillary electrophoresis (Attig et al., 2021), and high-performance liquid chromatography (HPLC) (Wolff et al., 2004). These analytical techniques have many disadvantages, such as involving expensive instruments and having complicated steps during sample preparation. Therefore, a sensitive, selective, and accurate method is needed to replace the analytical methods. Modern methods are considered cheaper, have a short detection time, are easy to handle, and are more portable compared to traditional detection methods. Modern detection methods include cyclic voltammetry (Hou et al., 2019), amperometry (Silva Junior et al., 2021), and impedance spectrometry (Kumaravel et al., 2021). Electrochemical sensors have been widely used for the detection of organic species, contaminants in the environment (Iqbal, 2020; Shanmugam et al., 2021; Sher et al., 2021) such as heavy metals (Jin et al., 2014), pesticides (Akyüz et al., 2019), and the composition of medicine. Electrochemical methods can reduce and oxidize analytes simultaneously. These methods have the ability to detect the contaminants with high selectivity and sensitivity (Shoaib et al., 2017; Bahadur et al., 2019; Bilge et al., 2021). In this view, modifying an electrode surface with appropriate nanoparticles that deliver excellent electrocatalytic capability to detect the pesticides on the electrode surface is a beneficial approach to fabricate a chemical sensor with excellent analytical performance. Numerous nano-materials, nano-tubes, and nano-composites have been studied in the reported literatures for the electrochemical detection of pesticides (Bolat and Abaci, 2018; Tian et al., 2018).

Polyatomic anions such as niobium, tungsten, vanadium, and molybdenum are transition metal oxides that may be utilized to build inorganic hybrid materials (27). The general formula of Polyoxometalate is XaMbOcn-; heteroatom X (Co, Si, Mn, P, and Fe, etc.) and metal M (Mo, W, V, and Nb, etc.) (28). Polyoxometalate (POM) are compounds of d-block transition metal coordinated with oxygen atoms (24). POM belongs to the inorganic metal oxides cluster family, and these metal oxides have a negative charge (25). POMs exist in an oxygen-rich complex with controllable size, shape, and charge (26). POMs can accept the numerous electrons giving rise to mixed-valence species and have the ability to connect with d–block transition metals at specific sides. These connections would apply to electronic, optical, and magnetic properties for making new substances (Baaalla et al., 2021). POMs have the dramatic capability to mix with water and some organic solvents, and on solid-state properties, they may be applied as homogenous catalysts (Vila-Nadal et al., 2012). The types of POM include Dawson, Kegging, Anderson, hourglass, and sandwich (Ying et al., 2019; Lan et al., 2020; Tian et al., 2020). POMs have many applications in different fields, such as acting as a photocatalyst for H_2

production (Gao et al., 2021). Protein-based POMs may be used for enhanced anti-bacterial activity in the biological field (Zhao et al., 2020) and in electrochemical studies for the detection of toxic compounds (Kowsalya et al., 2019). POMs may have been used for the fabrication of many types of substrates i.e., glassy carbon electrodes (GCEs) and screen-printed electrodes (SPEs). Various methods have been employed to fabricate POMs, including the layer-by-layer method (LBL) (Yaqub et al., 2022), electrochemical deposition method, Langmuir Blodgett method, and sol-gel process. The LBL method involves multilayer buildup by using both cationic and anionic species with alternate deposition (Ali et al., 2020). LBL method has been found suitable for the deposition of polyelectrolytes, control over film growth, and thickness of the film at the nanometer scale. By using this method the deposited films were mechanically robust and permeable for small molecules (Ammam, 2013).

In this article, we report that the active surface of the electrode with the fabrication of both anionic POM and cationic PEI-AgNPs was done by self-assembled layer-by-layer technique. The multilayer film was prepared by alternating depositions of cationic and anionic species and the composite film was characterized by UV-visible spectroscopy, FT-IR, XRD, AFM, and SEM. This hybrid film was used for the detection/sensing of targeted pesticides (MP) *via* the cyclic voltammetry technique. It has shown Dawson type Heteropolyoxoanions glassy carbon electrode sensor for detecting pesticides, which have multilayer films prepared by alternate deposition. These multilayer films show excellent electro-catalytic activity for detecting toxic compounds due to their nontoxic effects and eco-friendliness, which make it more applicable for future food safety and industrial and agricultural processes.

2 MATERIALS AND METHODS

2.1 Chemicals

The parent Dawson Polyoxometalate was synthesized according to the literature (Content et al., 1990). Sodium tungstate ($Na_2WO_4{\cdot}2H_2O$) (Sigma), orthophosphoric acid (85%) (H_3PO_4) (MERCK), ammonium chloride (NH_4Cl) (DAEJUNG), potassium chloride (KCl) (DAEJUNG), potassium hydrogen carbonate ($KHCO_3$) (MERCK), silver nitrate ($AgNO_3$) (CARIOERBA), polyethyleneimine (PEI) (Sigma Aldrich), and distilled water (Reservoir Elga) are all analytical grade chemicals that were used in the synthesis. Different electrolytes were prepared for electrochemical measurements (0.1M Na_2SO_4), (0.1M Na_2SO_4 + 20 mM CH_3CHOOH) and 0.04M Britton Robinson Buffer. Dawson/PDDA PEI-AgNPs fabricated GCE was prepared for electrochemical measurements (cyclic voltammetry) after purging/degassing of all buffers.

2.2 Preparation of Polyethyleneimine Stabilized Silver Nanoparticles

The current research is shown in **Scheme 1**. Silver nanoparticles (AgNPs) were prepared by dissolving silver nitrate (16.9 mg) in 10 ml distilled water followed by the addition of 300 µL polyethyleneimine (PEI). The solution container was wrapped entirely with covered aluminum foil and heated at 80°C until a light brown color appeared (40).

2.3 Electrochemical Procedure

Electrochemical studies were done on Gamry Potentiostat using a 3-electrode system. A glassy carbon electrode was

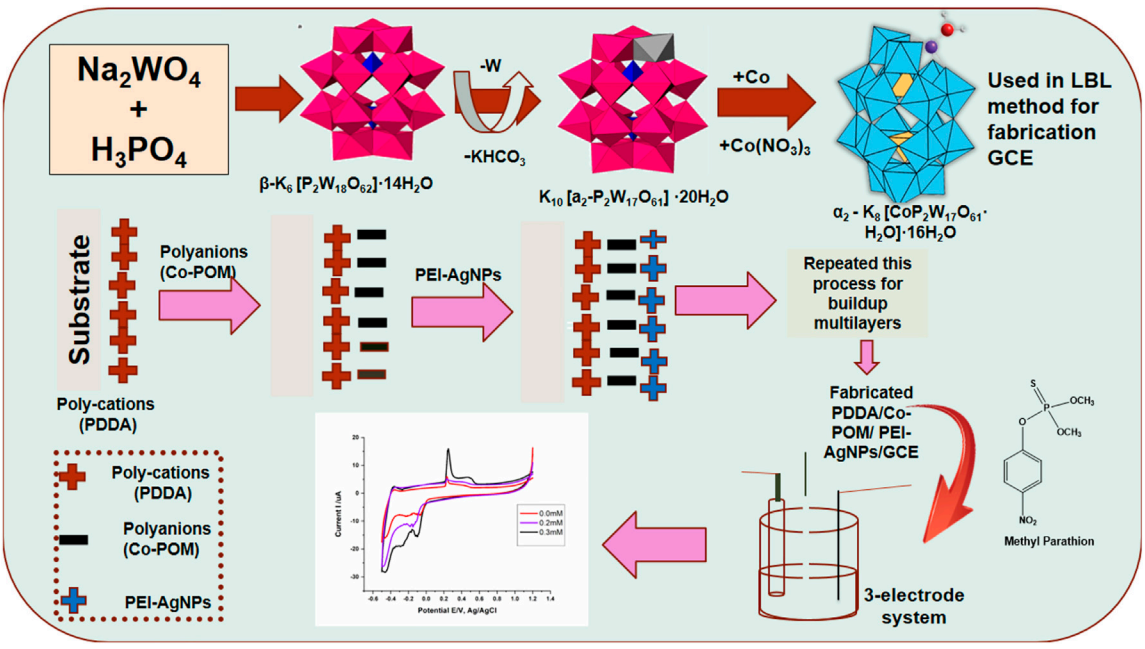

SCHEME 1 | The current investigation is shown in diagram form.

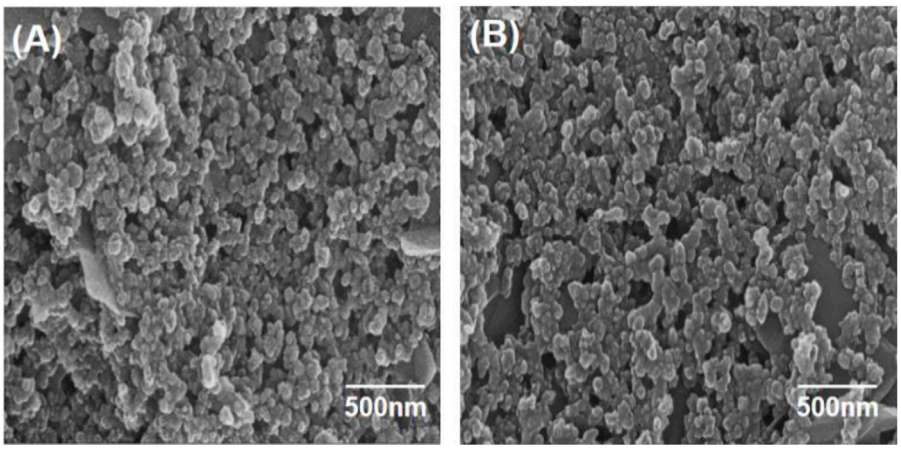

FIGURE 1 | SEM of multilayer assembly **(A)** outermost layer is AgNPs, **(B)** outermost layer is POM at 500 nm.

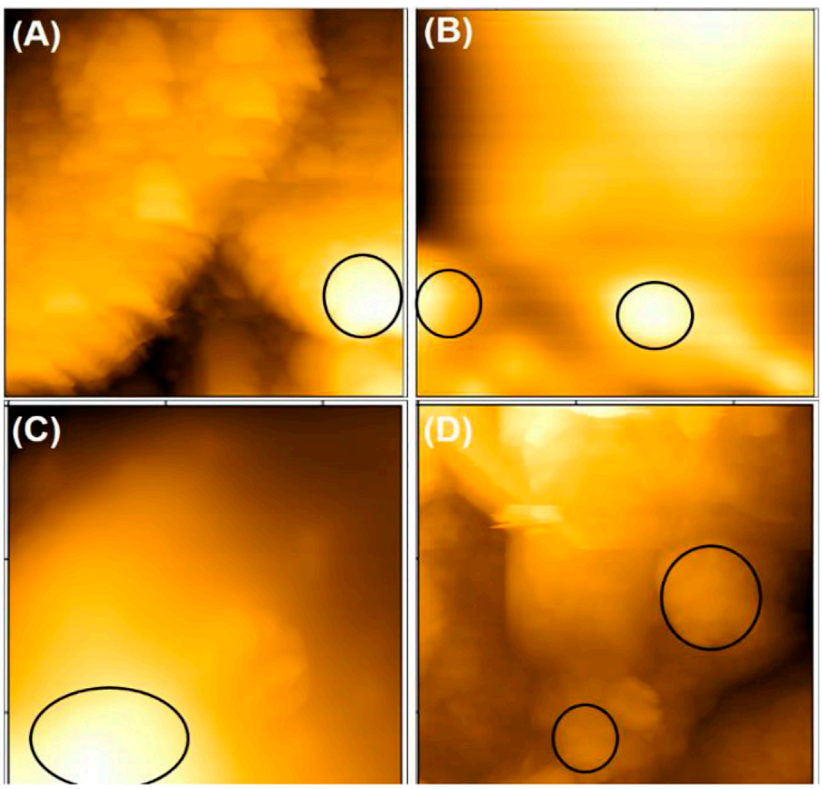

FIGURE 2 | AFM image; **(A)** Bare/SPE **(B)** PDDA/SCPE **(C)** PDDA/P_2W_{18} POM/PEI-AgNPs/SCPE with outer layer PEI-AgNPs **(D)** PDDA/PEI-AgNPs/P_2W_{18} POM/SCPE with outer layer of POM.

used as a working electrode. Silver-silver chloride (Ag/AgCl) electrode saturated in Potassium Chloride (KCl) was used as a reference electrode. Platinum wire was used as a counter for cyclic voltammetry characterization. Electrolytes were taken in the cell. All three electrodes (modified electrode that acts as working electrode, reference electrode, and counter electrode) were dipped in the cell. A glassy carbon electrode (GCE) was used as a working electrode and polished with alumina powder of 1.0, 0.3, and 0.05 micron, respectively. GCE was dipped in 0.5 ml polydimethyldiaylammomium chloride (PDDA) solution for 30 min and then slightly rinsed with distilled water after removing from PDDA solution. After that, the electrode was dipped in the metal substituted POM for 20 min. PDDA/Dawson POM-based modified electrode was again

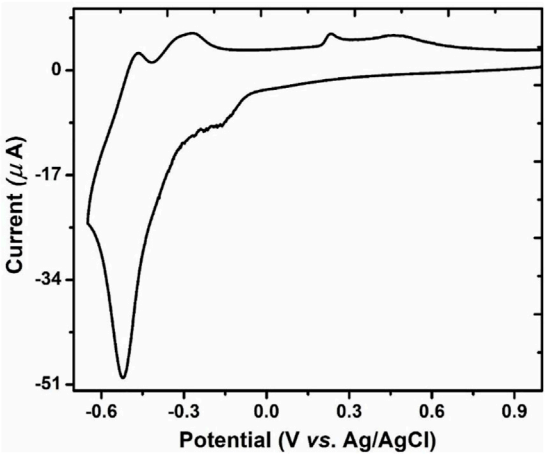

FIGURE 3 | CV of GCE, P_2W_{18} POM containing electrolyte in 0.1 M acetate buffer with scan rate 100 mVs^{-1}.

rinsed with distilled water to remove unwanted material. Then the modified electrode was dipped in 0.5 ml PEI-AgNPs for 20 min. The same procedure was followed to build up sixteen layers on the GCE.

2.4 Instrumentations

Ultra-violet visible characterization of synthesized silver nanoparticles was carried out by using a UV-Visible spectrophotometer (PARKEN ELMER LAMDA 750). Distilled water was used in the whole process. Fourier transform infrared analysis was performed on the Thermo Fisher Scientific FTIR and used for characterizing the synthesized Dawson POM in powder form. Scanning electron microscope (SEM) characterization was carried out by using NOVA NANO SEM at 500 nm. SEM characterized the multilayer formation of synthesized nanoparticles and Dawson POM. Multilayer formation was developed on the glassy carbon electrodes. X-ray diffraction determined the crystalline structure and phase and was carried out using Bruker D8 XRD. The structure of synthesized POM and buildup multilayers film on the active surface of the modified screen-printed electrode (SCPE) was also characterized *via* XRD. Atomic force microscope gave information about 3-D topography by using AFM-PARK XE7. Built up multilayers of Dawson POM and PEI stabilized AgNPs on SCPE for analysis.

3 RESULTS AND DISCUSSIONS

3.1 Characterization With Physical Methods

3.1.1 UV-Vis Spectroscopy Characterization

Using PEI solution, preparation and stabilization of silver nanoparticles were carried out to make chelate of transition metal ions (silver metal ions) with amino groups in PEI, which were confirmed by UV-vis spectroscopy. As shown in **Supplementary Figure S1**, the color change from colorless to brown solution confirmed the preparation of PEI-Ag NPs. UV-vis spectrum of PEI- Ag NPs exhibited the absorption (λ_{max}) peak at 430 nm which is in good agreement with data described in the literature (Kim et al., 2010; Imar et al., 2015; Wen et al., 2017).

3.1.2 FT-IR Studies

FTIR spectra exhibited characteristics vibration bands of Dawson Polyoxometalate compounds in 4000-500 cm^{-1}. The peak values revealed terminal W=O and v (P-O) vibrations, whereas bridge's vibrations of inter and intra tungstate-oxygen-tungstate (W-Ob-W) bands in the range of 700 and 900 cm^{-1} were presented in **Supplementary Table S1** (43). **Supplementary Figure S2** showed the physical appearance of Dawson-type POM. In **Supplementary Figure S3**, the characterization bands of heteropolyanions are between 700 and 1,100 cm^{-1}, which proved the Dawson structure.

3.1.3 X-Ray Diffraction Analysis

The spectra **Supplementary Figure S4** showed that the designed materials were in amorphous form and the main diffraction angles were recorded at 2 thetas (12°, 15°, 24°, 26°, 31°, 32°, 36°, 55°, and 53°) and two thetas (26.7°, 28.55°) for the Dawson POM and fabricated PDDA/P_2W_{18} POM/AgNPs/SCPE respectively. There was good agreement with the data described in the literature (Modvig et al., 2019). P_2W_{18} POM and PEI-AgNPs were used for multilayer formations on the screen-printed electrode (SCPE), and XRD characterization showed the amorphous structure of fabrication of PDDA/P_2W_{18} POM/PEI-AgNPs on the active surface of screen printed electrodes (SCPEs) with multilayers (Zhao et al., 2021).

3.1.4 Scanning Electron Microscope Studies

Changes in films morphology of fabricated samples with P_2W_{18} POM and PEI-AgNPs deposited on PDDA modified electrodes were examined via scanning electron microscope. SEM image of a

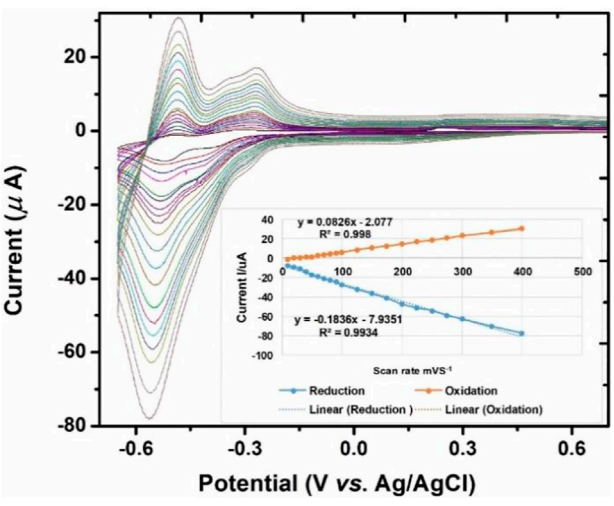

FIGURE 4 | CV of PDDA/P_2W_{18} POM/PEI-AgNPs/GCE in 0.1 M acetate buffer at different scan rates 10 to 400 mVs^{-1}.

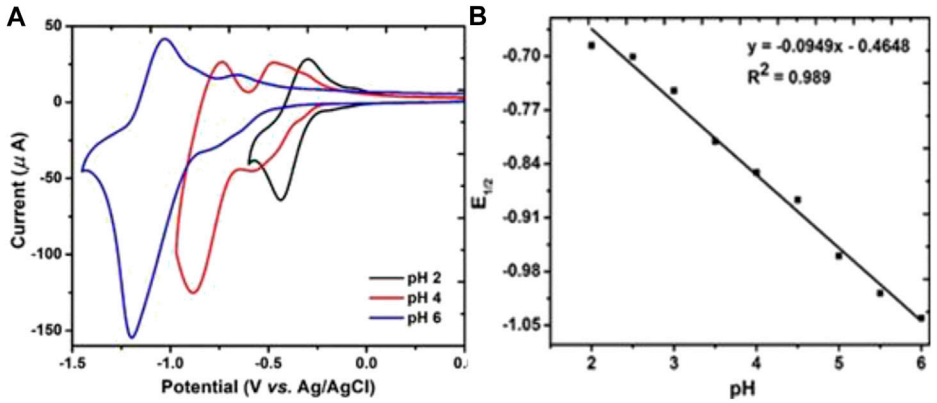

FIGURE 5 | (A) Cyclic voltammograms of multilayers assemblies of fabricated P_2W_{18} POM/AgNPs/GCE in pH 2, 4 and 6 (0.1M Acetate buffer) at scan rate 100mV/S.**(B)** pH versus reduction potential $E_{1/2}$.

TABLE 1 | pH study of fabricated P_2W_{18} POM/AgNPs/GCE.

pH	Cathodic peak E $_{pc}$ Sukirtha and Usharani (2013)	Anodic peak E $_{pa}$ Sukirtha and Usharani (2013)	$E_{1/2}$
2	−0.6199	−0.7599	−0.68599
2.5	−0.6537	−0.7479	−0.70085
3	−0.6839	−0.8058	−0.74485
3.5	−0.7179	−0.9639	−0.8109
4	−0.7399	−0.0893	−0.85119
4.5	−0.7539	−0.9198	−0.88685
5	−0.8059	−0.9939	−0.9599
5.5	−0.9979	−1.172	−1.00847
6	−1.032	−1.2	−1.0406

modified electrode with POM and PEI- AgNPs (outer layer) deposit film exhibits the aggregates with an average size of 500 nm, as shown in **Figure 1A**. SEM image of modified electrode PEI stabilized AgNPs and POM (outer layer) deposit film exhibit the construction of identical agglomerates with size is 500 nm, as shown in **Figure 1B**.

3.1.5 Atomic Force Microscope Studies

Surface images of Dawson POM and PEI-stabilized AgNPs deposited on screen-printed electrodes were performed by Atomic force microscope (AFM) and are shown in **Figure 2**. Atomic force microscope images were conducted at intervals throughout the multilayers *via* deposition method to investigate the variations in the topography during the process. Images of samples such as blank/SCPE (A), PDDA/SCPE (B), PDDA/cobalt substituted Dawson POM/PEI-AgNPs/SCPE with outer layer PEI-AgNPs (C), and PDDA/PEI-AgNPs/cobalt substituted Dawson POM/SCPE with outer layer cobalt substituted Dawson POM (D) were used to find the topography of the multilayers. An AFM image obtained with PDDA/SCPE has a more spherical structure indicative of polymeric film. These structures of all LBL films have a hemispherical shape (Anwar et al., 2014).

3.2 Electrochemical Measurements

3.2.1 Solution Electrochemistry

The electrochemical redox properties of cobalt substituted Dawson POM were recorded in 3 ml acetate buffer (0.1M Na_2SO_4 and 20 mM CH_3COOH) via cyclic voltammetry (CV) technique. One reversible redox pair I-I' exhibited and redox potential $E_{1/2}$ = (Epa + Epc) is—0.650 mV correlated with redox behavior of tungsten-oxo framework of (P_2W_{18}) Dawson type Polyoxometalate in cyclic voltammograms (Imar et al., 2015), which are shown in **Figure 3**.

$$[P_2W_{18}O_{62}]^{6-} + 2e^- + 2H^+ \rightleftharpoons [H_2P_2W_{18}O_{62}]^{6-}$$
$$[H_2P_2W_{18}O_{62}]^{6-} + 2e^- + 2H^+ \rightleftharpoons [H_4P_2W_{18}O_{62}]^{6-}$$

3.2.2 Multilayer Formations on Glassy Carbon Electrodes

The polydimethyldiallyammonium chloride (8% PDDA) was introduced to prepare glassy carbon electrodes (GCE). A glassy carbon electrode was polished with alumina powder and dipped in 0.5 ml 8% PDDA solution (polycations). CV was recorded in 10 ml acetate buffer pH 3.5 in **Supplementary Figure S5A**. Multilayer formation depends on cationic and anionic moieties. Multilayers were built up with P_2W_{18} POM and AgNPs stabilized with polyethyleneimine on PDDA/GCE modified electrode with layer-by -layer (LBL) method and degassing with nitrogen gas before each layer formation. CV was recorded in 0.1 M acetate buffer pH 3.5 at a scan rate of 100 mV/S after formation. In multilayer formation, the outermost layer was P_2W_{18} Dawson Polyoxometalate, anionic moieties. In **Supplementary Figure S5B**, the peak of current (*u*A) increases gradually in the redox couple I, increasing the number of layers and decreasing peak to peak separation in recorded CV. The incorporative AgNPs exhibited a small increase in the current peak during the construction of multilayers. A slight anodic shift was examined for the W-O redox process with layer-by-layer assembly immobilization associated with the POM solution response, which demonstrated the interactions between POM and PEI-stabilized AgNPs within the construction of multilayers (Anwar et al., 2014).

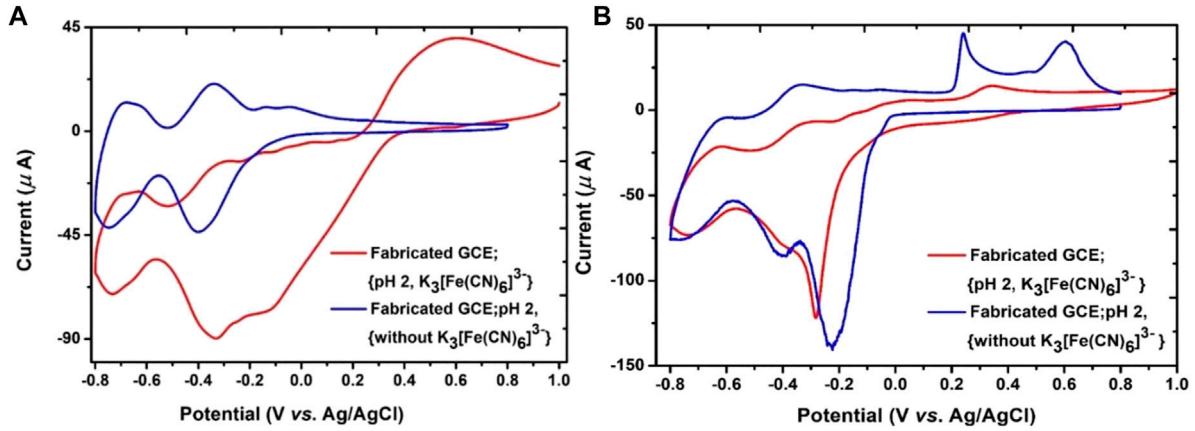

FIGURE 6 | (A) Permeability of P_2W_{18} POM towards $K_3Fe(CN)_6$ redox probe diffusion. Cyclic voltammograms were recorded at pH 2 acetate buffer, Scan rate 100 mVS^{-1} before and after added layer. **(B)** Fabricated GCE (16 multilayers) with the anionic outermost layer. Scan rate 100mV/S.

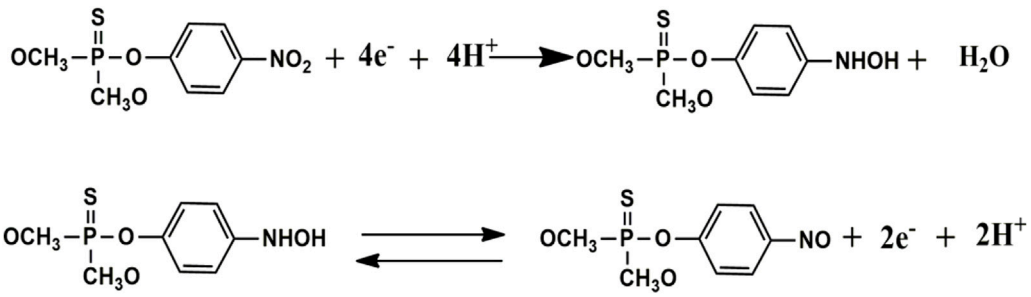

FIGURE 7 | Chemical mechanism of methyl parathion reduction.

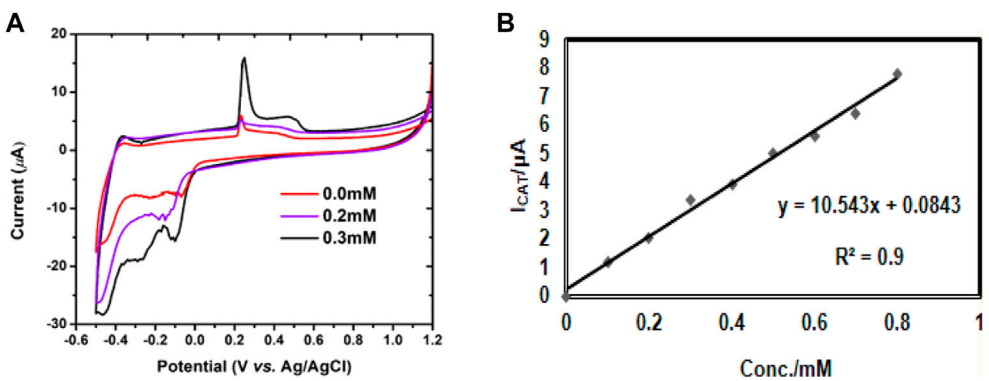

FIGURE 8 | (A) Methyl Parathion catalysis on the P_2W_{18} Polyoxometalate LBL composite films. CV of P_2W_{18} Polyoxometalate-AgNPs multilayer in each step was recorded before adding analyte (black) curve and after adding analyte; (0.2–2.0 mM), pH 4.5, and scan rate 10mV/S. **(B)** Electro-catalytic for detection of methyl parathion on LBL film of P_2W_{18} POM with multilayers.

3.2.3 Scan Rate Study

For scan rate study, a glassy carbon electrode was modified with P2W18 POM and PEI-AgNPs. After making multilayers, a scan rate study of fabricated P_2W_{18} POM/AgNPs/GCE modified electrode was carried out via cyclic voltammetry. 0.1 M acetate buffer, pH 3.5 was used in the 3-electrode system. **Figure 4** shows cyclic voltammograms of multilayers of PDDA/POM/AgNPs at 10 to 400 scan rate mVS^{-1} on GCE. In cyclic voltammograms,

redox couples exhibited a gradual change in oxidation and reduction peaks. Scan rate study depends on the anionic moieties (POM as the outermost layer). The current was increased with the increase of scan rate mVS^{-1}.

3.2.4 pH Study

The pH study of P_2W_{18} POM depends on the pH of the buffer. In electrochemical measurements, reduction of P_2W_{18} POM went together with protonation. Oxidation and reduction peaks of P_2W_{18} POM vary with the pH of the buffer. Therefore, the electrochemical study was pH-dependent. Three different types of acetate buffers were prepared for pH study. The first acetate buffer was 0.1 M Na_2SO_4 at (pH = 2, 2.5, and 3). The second acetate buffer was 0.1M Na_2SO_4 and 20 mM CH_3COOH at (pH = 3.5, 4, 4.5, and 5). The third was 0.1M Na_2SO_4 and $Na_2H_2PO_4$ at (pH = 5.5 and 6). All pH studies were carried out *via* the cyclic voltammetry technique. **Figure 5A** presents fabricated P2W18 POM/PEI-AgNPs/GCE, which was used for pH studies at a scan rate of 100 mVS^{-1}. It was discovered that film showed the stable redox activity linked with Tungsten-oxo centers within Dawson POM between pH ranges 2 to 6 based on acetate buffers solution. Dawson POM exhibited a redox process and shifted cathodically with the pH increase and the number of protons linked with each redox process. In **Figure 5B**, the current decreases when the pH value of the electrolyte increases. The resulting slope value of Dawson POM was examined at 0.017 mV/pH due to the addition of proton per monoelectronic redox process in solution (Anwar et al., 2014; Zhou et al., 2021). Calculated $E_{1/2}$ values at different pH are presented in **Table 1** (Sukirtha and Usharani, 2013).

3.2.5 Permeability of Layer-By-Layer Films

The permeability of layer-by-layer (LBL) films was investigated through cyclic voltammetry (CV) towards cationic and anionic redox probes, such as potassium ferricyanide $K_3[Fe(CN)_6]$, and characterized by monoelectronic redox process. Redox transformations occurred on the electrode surface or within LBL film after diffusion by the redox probe. **Figure 6A** exhibited the cyclic voltammogram of bare GCE and fabricated GCE with PDDA, P_2W_{18} POM, and PEI-AgNPs layer-by-layer film depending on the number of layers and outermost layer (Fay et al., 2005). Fe $(CN)_6$ can penetrate the multilayers and react at the bare GCE. Repulsion produced between the outer anionic layer and Fe (CN)6 significantly increases the peak-to-peak separation. Fabricated GCE with LBL films led to suppressing the redox probes' peaks, which created difficulty for the probe for diffusion in the layer-by-layer (LBL) films at the GCE. Surface permeability of fabricated GCE (eight multilayers) with cationic PEI-AgNPs (outermost layer) exhibited redox activity of the anionic probe at the GCE due to electrostatic interactions between the anionic probe and cationic layer (outermost layer).

In **Figure 6B**, fabricated GCE (16 multilayers) with anionic POM (outermost layer) showed no redox activity due to unfavorable electrostatic repulsion between the anionic probe and outermost layer. The cathodic current increased the redox processes by increasing film thickness determined in the presence of anionic probe, resulting in electrocatalytic reduction due to electron transfer from cationic species (Naseer et al., 2015). The experiment was carried out in 0.1 M acetate buffer at pH 2, 0.1M Na_2SO_4, and 1 mM Potassium ferricyanide $K_3[Fe(CN)_6]$ solution was prepared for permeability at scan rate 100 mV/S (Anwar et al., 2014). A small reduction in current peaks associated with the redox process of the electrode can be investigated with the increase in peak-to-peak separation on fabricated GCE while decreases in peak-to-peak separation can be seen on bare GCE (Imar et al., 2015).

3.2.6 Electrochemical Response of P2W18 Polyoxometalate

The electrochemical performance of P_2W_{18} Polyoxometalate towards methyl parathion was investigated in 0.04 M Britton Robison Buffer at pH 4.5 via cyclic voltammetry. Chemical mechanism of methyl parathion reduction is given in **Figure 7**. **Figure 8A** shows the CV curve of P_2W_{18} Polyoxometalate in the presence and absence of methyl parathion along with fabricated PDDA/P_2W_{18} POM/PEI-AgNPs/GCE. With the addition of 20 μL methyl parathion, the reduction peak current increases gradually. The penetration of transition centers with heteropolyanions enhanced the catalytic behavior and generated highly reduced products by the electrons from the reduced W-O framework. These results exhibited a reduced form of HPA that catalyzes the methyl parathion reduction. Catalytic current peak (−0.7V) increased with the increase of MP concentration. Sensitivities were assessed with a linear range of 0.2–2.0 mM. The detection limit was achieved at 29 μM methyl parathion detection at LBL composite PDDA, P_2W_{18} and PEI-AgNPs and showed the limit of detection was found at 1 ppm (Hou et al., 2019). In **Figure 8B**, the reduction current peak increases with the addition of the concentration of the analyte. The reduction current peak is directly proportional to the concentration of methyl parathion.

4 CONCLUSION

This study used a layer-by-layer method for the electrostatic deposition of cationic PEI-AgNPs and anionic POM species. The newly prepared composite film was thoroughly characterized by UV-Vis, FT-IR, XRD, AFM, and SEM techniques. The colorless solution of PEI turned to brown after adding the silver nitrate, which was due to the complex formation of Ag^+ with the functional group (amino) of PEI, resulting in PEI-AgNPs that was confirmed by the presence of absorption peak at 430 nm in the UV-Vis spectroscopy. FT-IR studies revealed that the peak at 884 cm^{-1} corresponded to W- O_c -W of Dawson POM. XRD analyses showed that the amorphous structure was formed by applying LBL fabrication of composite films. Surface images of composite films were obtained by AFM, which showed that the structures of all LBL composites films have a hemispherical shape. SEM results showed that composite films exhibited the construction of identical agglomerates with size 500 nm. The results of all the characterizations showed that composite film was successfully synthesized. Furthermore, all electrochemical measurements were studied by using CV. The composite film showed pH-dependent redox behavior within the pH range (2–6) and exhibited excellent stable redox properties towards P_2W_{18}

POM. The LBL composite film was also investigated for its catalytic efficiency towards the detection of methyl parathion. The electrocatalysis exhibited the current response for the detection of methyl parathion and was found at less than 1 ppm. This LBL composite film was fruitfully applied for the detection of pesticide (MP).

DATA AVAILABILITY STATEMENT

The original contributions presented in the study are included in the article/**Supplementary Material**, further inquiries can be directed to the corresponding authors.

AUTHOR CONTRIBUTIONS

NAD: Visualization of data, reviewed the original manuscript and critical revision. MY: Interpret the data, writing-original draft preparation. SN: Conception, design of the study, writing-original draft preparation. SJ: Conception, design of the study, acquisition of data. SUH: Visualization of data, reviewed the original manuscript. MJ: Conception, design of the study, acquisition of data, interpret the data. SI: Interpret the data, performed major experimental works, writing-original draft preparation and editing. EBE: Financial funding, visualization of data. FHA: Interpret the data, and critical revision. NA: Reviewed original manuscript, and critical revision. RMA: Reviewed original manuscript, and critical revision. NSA: Visualization of data, CV analysis, writing reviewing and editing. HAI: Conception, visualization of data, performed CV analysis, acquisition of data.

ACKNOWLEDGMENTS

The authors extend their appreciation to the Deanship of Scientific Research at King Khalid University for supporting this work through research groups program under grant number R.G.P.2/120/42. RA would like to acknowledge Taif University Researchers Supporting Project Number (TURSP-2020/209), Taif University, Taif, Saudi Arabia. The authors extend their appreciation to the Research Center at AlMaarefa University for funding this work.

SUPPLEMENTARY MATERIAL

The Supplementary Material for this article can be found online at: https://www.frontiersin.org/articles/10.3389/fmats.2022.877683/full#supplementary-material

REFERENCES

Aktar, W., Sengupta, D., and Chowdhury, A. (2009). Impact of Pesticides Use in Agriculture: Their Benefits and Hazards. *Interdiscip. Toxicol.* 2, 1–12. doi:10.2478/v10102-009-0001-7

Akyüz, D., Koca, A., and Chemical, A. B. (2019). An Electrochemical Sensor for the Detection of Pesticides Based on the Hybrid of Manganese Phthalocyanine and Polyaniline. *Sensors Actuators B: Chem.* 283, 848–856. doi:10.1016/j.snb.2018.11.155

Ali, B., Mccormac, T., Maccato, C., Barreca, D., and Carraro, G. (2020). Multilayer Assemblies of a Cu-Phthalocyanine with Dawson Type Polyoxometalates (POMs) for the Electrocatalytic Reduction of Phosphate. *J. Electroanalytical Chem.* 858, 113770. doi:10.1016/j.jelechem.2019.113770

Ammam, M. (2013). Polyoxometalates: Formation, Structures, Principal Properties, Main Deposition Methods and Application in Sensing. *J. Mater. Chem. A.* 1, 6291–6312. doi:10.1039/c3ta01663c

Anwar, N., Sartorel, A., Yaqub, M., Wearen, K., Laffir, F., Armstrong, G., et al. (2014). Surface Immobilization of a Tetra-Ruthenium Substituted Polyoxometalate Water Oxidation Catalyst through the Employment of Conducting Polypyrrole and the Layer-By-Layer (LBL) Technique. *ACS Appl. Mater. Inter.* 6, 8022–8031. doi:10.1021/am405295c

Baaalla, N., Ammari, Y., Hlil, E. K., Abid, S., Masrour, R., Benyoussef, A., et al. (2021). The Novel Material Based on Strandberg-type Hybrid Complex (C6H10N2)2[Co(H2O)4P2Mo5O23].6H2O: Experimental and Simulations Investigation on Electronic, Optical, and Magnetocaloric Properties. *Ceramics Int.* 47, 2338–2346. doi:10.1016/j.ceramint.2020.09.076

Bahadur, A., Saeed, A., Shoaib, M., Iqbal, S., and Anwer, S. (2019). Modulating the Burst Drug Release Effect of Waterborne Polyurethane Matrix by Modifying with Polymethylmethacrylate. *J. Appl. Polym. Sci.* 136, 47253. doi:10.1002/app.47253

Ben Attig, J., Latrous, L., Zougagh, M., and Ríos, Á. (2021). Ionic Liquid and Magnetic Multiwalled Carbon Nanotubes for Extraction of N-Methylcarbamate Pesticides from Water Samples Prior Their Determination by Capillary Electrophoresis. *Talant.a* 226, 122106. doi:10.1016/j.talanta.2021.122106

Bilge, S., Dogan-Topal, B., Atici, E. B., Sınağ, A., Ozkan, S. A., and Chemical, A. B. (2021). Rod-like CuO Nanoparticles/waste Masks Carbon Modified Glassy Carbon Electrode as a Voltammetric Nanosensor for the Sensitive Determination of Anti-cancer Drug Pazopanib in Biological and Pharmaceutical Samples. *Sensors Actuators B: Chem.* 343, 130109. doi:10.1016/j.snb.2021.130109

Bolat, G., and Abaci, S. (2018). Non-enzymatic Electrochemical Sensing of Malathion Pesticide in Tomato and Apple Samples Based on Gold Nanoparticles-Chitosan-Ionic Liquid Hybrid Nanocomposite. *Sensors.* 18, 773. doi:10.3390/s18030773

Facure, M. H. M., Mercante, L. A., Mattoso, L. H. C., and Correa, D. S. (2017). Detection of Trace Levels of Organophosphate Pesticides Using an Electronic Tongue Based on Graphene Hybrid Nanocomposites. *Talanta.* 167, 59–66. doi:10.1016/j.talanta.2017.02.005

Fay, N., Dempsey, E., and Mccormac, T. (2005). Assembly, Electrochemical Characterisation and Electrocatalytic Ability of Multilayer Films Based on [Fe(bpy)3]2+, and the Dawson Heteropolyanion, [P2W18O62]6–. *J. Electroanalytical Chem.* 574, 359–366. doi:10.1016/j.jelechem.2004.07.038

Febbraio, F., Merone, L., Cetrangolo, G. P., Rossi, M., Nucci, R., and Manco, G. (2011). Thermostable Esterase 2 from Alicyclobacillus Acidocaldarius as Biosensor for the Detection of Organophosphate Pesticides. *Anal. Chem.* 83, 1530–1536. doi:10.1021/ac102025z

Gao, X., Wang, J., Xue, Q., Ma, Y.-Y., and Gao, Y. (2021). AgBr/Polyoxometalate/Graphene Oxide Ternary Composites for Visible Light-Driven Photocatalytic Hydrogen Production. *ACS Appl. Nano Mater.* 4, 2126–2135. doi:10.1021/acsanm.0c03406

Hassaan, M. A., and El Nemr, A. J. T. E. J. O. a. R. (2020). Pesticides Pollution: Classifications, Human Health Impact, Extraction and Treatment Techniques. *Egypt. J. Aquat. Res.* 46 (3), 207–220. doi:10.1016/j.ejar.2020.08.007

Hou, X., Liu, X., Li, Z., Zhang, J., Du, G., Ran, X., et al. (2019). Electrochemical Determination of Methyl Parathion Based on pillar[5]arene@AuNPs@reduced Graphene Oxide Hybrid Nanomaterials. *New J. Chem.* 43, 13048–13057. doi:10.1039/c9nj02901j

Hussain, A., Audira, G., Malhotra, N., Uapipatanakul, B., Chen, J.-R., Lai, Y.-H., et al. (2020). Multiple Screening of Pesticides Toxicity in Zebrafish and daphnia Based on Locomotor Activity Alterations. *Biomolecules.* 10, 1224. doi:10.3390/biom10091224

Imar, S., Yaqub, M., Maccato, C., Dickinson, C., Laffir, F., Vagin, M., et al. (2015). Nitrate and Nitrite Electrocatalytic Reduction at Layer-By-Layer Films Composed of Dawson-type Heteropolyanions Mono-Substituted with

Transitional Metal Ions and Silver Nanoparticles. *Electrochimica Acta.* 184, 323–330. doi:10.1016/j.electacta.2015.10.082

Iqbal, S. (2020). Spatial Charge Separation and Transfer in L-Cysteine Capped NiCoP/CdS Nano-Heterojunction Activated with Intimate Covalent Bonding for High-Quantum-Yield Photocatalytic Hydrogen Evolution. *Appl. Catal. B: Environ.* 274, 119097. doi:10.1016/j.apcatb.2020.119097

Jin, W., Wu, G., and Chen, A. (2014). Sensitive and Selective Electrochemical Detection of Chromium(vi) Based on Gold Nanoparticle-Decorated Titania Nanotube Arrays. *Analyst.* 139, 235–241. doi:10.1039/c3an01614e

Kim, K., Lee, H. B., Lee, J. W., Shin, K. S., and Science, I. (2010). Poly(ethylenimine)-stabilized Silver Nanoparticles Assembled into 2-dimensional Arrays at Water-Toluene Interface. *J. Colloid Interf. Sci.* 345, 103–108. doi:10.1016/j.jcis.2010.01.039

Kowsalya, B., Anusha Thampi, V. V., Sivakumar, V., and Subramanian, B. (2019). Electrochemical Detection of Chromium(VI) Using NiO Nanoparticles. *J. Mater. Sci. Mater. Electron.* 30, 14755–14761. doi:10.1007/s10854-019-01847-3

Kumaravel, A., Murugananthan, M., and Chemical, A. B. (2021). Electrochemical Detection of Fenitrothion Usingnanosilver/dodecane Modified Glassy Carbon Electrode. *Sensors Actuators B: Chem.* 331, 129467. doi:10.1016/j.snb.2021.129467

Lan, Q., Dou, T.-T., Jin, S.-J., and Zhang, Z.-M. (2020). Design and Synthesis of {CaCo3}-Based sandwich-type Polyoxometalate. *J. Coord. Chem.* 73, 2373–2382. doi:10.1080/00958972.2020.1799198

Luo, L., Dong, L., Huang, Q., Ma, S., Fantke, P., Li, J., et al. (2021). Detection and Risk Assessments of Multi-Pesticides in 1771 Cultivated Herbal Medicines by LC/MS-MS and GC/MS-MS. *Chemosphere.* 262, 127477. doi:10.1016/j.chemosphere.2020.127477

Modvig, A., Kumpidet, C., Riisager, A., and Albert, J. (2019). Ru-Doped Wells-Dawson Polyoxometalate as Efficient Catalyst for Glycerol Hydrogenolysis to Propanediols. *Materials.* 12, 2175. doi:10.3390/ma12132175

Naseer, R., Mal, S. S., Kortz, U., Armstrong, G., Laffir, F., Dickinson, C., et al. (2015). Electrocatalysis by crown-type Polyoxometalates Multi-Substituted by Transition Metal Ions; Comparative Study. *Electrochimica Acta.* 176, 1248–1255. doi:10.1016/j.electacta.2015.07.152

Negatu, B., Kromhout, H., Mekonnen, Y., and Vermeulen, R. (2016). Use of Chemical Pesticides in Ethiopia: a Cross-Sectional Comparative Study on Knowledge, Attitude and Practice of Farmers and Farm Workers in Three Farming Systems. *Annhyg.* 60, 551–566. doi:10.1093/annhyg/mew004

Oultaf, L., Metna Ali Ahmed, F., and Sadoudi Ali Ahmed, D. (2022). Environmental and Health Risks of Pesticide Use Practices by Farmers in the Region of Tizi-Ouzou (Northern Algeria). *Int. J. Environ. Stud.* 79, 1–11. doi:10.1080/00207233.2022.2044693

Parham, H., and Rahbar, N. (2010). Square Wave Voltammetric Determination of Methyl Parathion Using ZrO2-Nanoparticles Modified Carbon Paste Electrode. *J. Hazard. Mater.* 177, 1077–1084. doi:10.1016/j.jhazmat.2010.01.031

Shanmugam, R., Alagumalai, K., Chen, S.-M., and Ganesan, T. (2021). Electrochemical Evaluation of Organic Pollutant Estradiol in Industrial Effluents. *J. Environ. Chem. Eng.* 9, 105723. doi:10.1016/j.jece.2021.105723

Sher, M. J., Shahid, S., Iqbal, S., Qamar, M. A., and BahadurQayyum, A. (2021). The Controlled Synthesis of G-C3N4/Cd-Doped ZnO Nanocomposites as Potential Photocatalysts for the Disinfection and Degradation of Organic Pollutants under Visible Light Irradiation. *J. Rsc Adv.* 11, 2025–2039. doi:10.1039/D0RA08573A

Shoaib, M., Bahadur, A., Rahman, M. S., Iqbal, S., Arshad, M. I., Tahir, M. A., et al. (2017). Sustained Drug Delivery of Doxorubicin as a Function of pH, Releasing media, and NCO Contents in Polyurethane Urea Elastomers. *J. Drug Deliv. Sci. Technology* 39, 277–282. doi:10.1016/j.jddst.2017.04.010

Silva Junior, G. J., Selva, J. S. G., Sukeri, A., Gonçalves, J. M., Regiart, M., and Bertotti, M. (2021). Fabrication of Dendritic Nanoporous Gold via a Two-step Amperometric Approach: Application for Electrochemical Detection of Methyl Parathion in River Water Samples. *Talanta.* 226, 122130. doi:10.1016/j.talanta.2021.122130

Sousa, S., Pestana, D., Faria, G., Vasconcelos, F., Delerue-Matos, C., Calhau, C., et al. (2020). Method Development for the Determination of Synthetic Musks and Organophosphorus Pesticides in Human Adipose Tissue. *J. Pharm. Biomed. Anal.* 191, 113598. doi:10.1016/j.jpba.2020.113598

Sukirtha, T., and Usharani, M. J. J. O. B.Biodegradation (2013). Production and Qualitative Analysis of Biosurfactant and Biodegradation of the Organophosphate by Nocardia Mediterranie. *J. Bioremediation Biodegradation.* 4, 198.

Tian, X., Liu, L., Li, Y., Yang, C., Zhou, Z., Nie, Y., et al. (2018). Nonenzymatic Electrochemical Sensor Based on CuO-TiO2 for Sensitive and Selective Detection of Methyl Parathion Pesticide in Ground Water. *Sensors Actuators B: Chem.* 256, 135–142. doi:10.1016/j.snb.2017.10.066

Tian, X., Zhang, Y., Ma, Y., Zhao, Q., and Han, Z.Technology (2020). Hourglass-type Polyoxometalate-Based Crystalline Materials as Efficient Cooperating Photocatalysts for the Reduction of Cr(vi) and Oxidation of Dyes. *Catal. Sci. Technol.* 10, 2593–2601. doi:10.1039/d0cy00208a

Van Den Berg, J., Greyvenstein, B., and Du Plessis, H. J. C. O. I. I. S. (2022). *Insect Resistance Management Facing African Smallholder Farmers under Climate Change.* Netherlands: Elsevier BV.

Vilà-Nadal, L., Romo, S., López, X., and Poblet, J. M. (2012). "Structural and Electronic Features of Wells-Dawson Polyoxometalates," in *Complexity in Chemistry and Beyond: Interplay Theory and Experiment* (Springer), 171–183. doi:10.1007/978-94-007-5548-2_10

Wen, T., Qu, F., Li, N. B., and Luo, H. Q. (2017). A Facile, Sensitive, and Rapid Spectrophotometric Method for Copper(II) Ion Detection in Aqueous media Using Polyethyleneimine. *Arabian J. Chem.* 10, S1680–S1685. doi:10.1016/j.arabjc.2013.06.013

Wolff, M., Builes, A., Zapata, G., Morales, G., and Benecke, M. J.Toxicology (2004). Detection of Parathion (O, O-Diethyl O-(4-nitrophenyl) Phosphorothioate) by HPLC in Insects of Forensic Importance in Medellín, Colombia. *Anil Aggrawal's Internet J. Forensic Med. Toxicol.* 5, 6–11.

Yaqub, A., Gilani, S. R., Bilal, S., Hayat, A., Asif, A., and Siddique, S. a. J. a. O. (2022). *Efficient Preparation of a Nonenzymatic Nanoassembly Based on Cobalt-Substituted Polyoxometalate and Polyethylene Imine-Capped Silver Nanoparticles for the Electrochemical Sensing of Carbofuran*. Washington, DC: American Chemical Society.

Ying, J., Chen, Y.-G., and Wang, X.-Y. (2019). A Series of 0D to 3D Anderson-type Polyoxometalate-Based Compounds Obtained under Ambient and Hydrothermal Conditions. *CrystEngComm* 21, 1168–1179. doi:10.1039/c8ce01971a

Zhao, H.-Y., Li, J.-Y., Dong, D.-P., and Wang, L. (2021). Two New Hybrids Built upon Wells-Dawson Polyoxoanions and Copper-Ethylendiamine Coordination Cations. *J. Mol. Struct.* 1239, 130387. doi:10.1016/j.molstruc.2021.130387

Zhao, M., Fang, Y., Ma, L., Zhu, X., Jiang, L., Li, M., et al. (2020). Synthesis, Characterization and *In Vitro* Antibacterial Mechanism Study of Two Keggin-type Polyoxometalates. *J. Inorg. Biochem.* 210, 111131. doi:10.1016/j.jinorgbio.2020.111131

Zheng, W., Luo, B., and Hu, X. (2020). The Determinants of Farmers' Fertilizers and Pesticides Use Behavior in China: An Explanation Based on Label Effect. *J. Clean. Prod.* 272, 123054. doi:10.1016/j.jclepro.2020.123054

Zhou, Q., Du, Y., Qu, Z., and Bi, L. (2021). Facile Multilayer Assemble of a Mixed-Valence Mn4-Containing Silicotungstate and its Electrochemical Study with Co3O4 as Co-catalyst for Photoelectrocatalytic Water Oxidation. *J. Electroanalytical Chem.* 894, 115339. doi:10.1016/j.jelechem.2021.115339

Conflict of Interest: The authors declare that the research was conducted in the absence of any commercial or financial relationships that could be construed as a potential conflict of interest.

Publisher's Note: All claims expressed in this article are solely those of the authors and do not necessarily represent those of their affiliated organizations, or those of the publisher, the editors and the reviewers. Any product that may be evaluated in this article, or claim that may be made by its manufacturer, is not guaranteed or endorsed by the publisher.